Magnetic Gearing Research at NASA

Vivake Asnani
Research Engineer
NASA Glenn Research Center
Cleveland, OH, USA

Justin Scheidler
Research Engineer
NASA Glenn Research Center
Cleveland, OH, USA

Thomas Tallerico
Research Engineer
NASA Glenn Research Center
Cleveland, OH, USA

ABSTRACT

Magnetic gearing is an alternative to mechanical gearing, where torque is transferred through magnetic force as opposed to contact force. The technology has the potential to be used in aircraft applications, without the lubrication, noise, and maintenance issues that can exist with mechanical gearing. Initial design and prototype development work was done at NASA to create a foundational understanding of the technology and the factors that influence its specific torque. The specific torque achieved through design optimization was found to be less than that of high-torque mechanical aircraft transmissions, but may be comparable to that of lower torque mechanical transmissions for electrified vertical takeoff and landing aircraft. The lessons learned from NASA's initial technology development and the direction of NASA's future work in field are discussed.

INTRODUCTION

It was recognized over 100 years ago that magnetic forces could be used to transmit torque in gears instead of mechanical tooth contact (Ref. 1). Gear tooth contact is the driver of several issues associated with traditional mechanical gears in vertical takeoff and landing (VTOL) vehicles. The most notable issues are friction-induced heating, wear, the potential for tooth failure, and high-frequency vibration excitation (Refs. 2, 3, and 4). These issues create three system-level consequences: 1) A lubrication system is needed to reduce the tooth friction and remove the generated heat. Typically, a backup system is also required to meet certification requirements for loss of lubrication performance (Ref. 5); 2) The level of cabin noise, which results from the gear tooth vibration, far exceeds that of alternative forms of transportation and necessitates the use of headsets for communication (Ref. 6); and 3) To mitigate tooth wear and failure, VTOL aircraft are grounded periodically for inspection and maintenance. Magnetic gearing, with its use of magnetic forces instead of tooth contact, has the potential to eliminate all these issues. However, even with recent advances in magnetic gear design and magnetic materials (Refs. 7 and 8), the maximum torque to mass ratio (specific torque) does not appear to be high enough to be competitive with mechanical gearboxes in traditional VTOL applications.

The emergence of point-to-point, origin-to-destination aircraft, has driven a new design space of VTOL vehicle propulsion architectures. Many vehicles make use of distributed electric propulsors for aerodynamic efficiency gains (Ref. 9). Smaller aircrafts and smaller propulsors, have reduced the powertrain torque requirements. Extrapolation of the trends in aircraft gearing (Ref. 10) shows that mechanical gearboxes will have reduced specific torque at these lower torque levels. As a result magnetic gearing is a more viable alternative in this market.

Due to the aforementioned issues with mechanical gearing, most emerging electrified vertical takeoff and landing (eVTOL) vehicles make use of direct drive motors, instead of geared motors. This limits the electric motor speed to below optimum levels due to aerodynamic constraints on the speed of the propeller. Electric motors can be made significantly lighter and/or more efficient if they are optimized to operate at higher speed and lower torque (Refs. 9, 11, and 12). Magnetic gearing could enable this optimization without the issues associated with mechanical gearing, providing range and payload capacity to these vehicles

The potential benefits for eVTOL and other aerospace applications has led NASA to start a 2-1/2 year project to develop a core competency in magnet gearing. There are three phases to the project. The first focuses on gaining a core understanding of the technology and increasing its specific torque. The second focuses on issues related to high speed operation of magnetic gears. The third phase addresses the issue of motor and magnetic gear integration. The purpose of this paper is to describe the technology advancements and lessons learned through phase one of the project, as well as thoughts on the technology development needs for eVTOL applications.

Presented at the AHS International 74th Annual Forum & Technology Display, Phoenix, Arizona, USA, May 14-17, 2018.

PRINCIPLES OF OPERATION

Some general principles of magnetic gearing technology are described here to provide a framework for the discussion to follow. For a broader overview, refer to Refs. (7 and 8). Like mechanical gears, magnetic gears can take many forms. Early designs were essentially patterned after mechanical gearing, where gear teeth were replaced by permanent magnets. As such, a force was transferred in the gear mesh through attractive and repulsive forces between magnet poles. These mechanical-equivalent magnetic gear topologies had significantly lower torque densities than their mechanical equivalents.[a] This is because the force carrying capacity of a single magnetic mesh is significantly less than that of a single mechanical mesh of similar size.

A major advancement of the technology was realized with the invention of the concentric magnetic gear (CMG) (Ref. 13) and the mathematics that enable its design for high torque density (Ref. 14). The topology of the CMG is analogous to that of a mechanical planetary gear set. It has two permanent magnet members that contain different numbers of poles and behave like the ring and sun gears of a mechanical planetary. A flux modulator, located in-between the magnetic ring and sun gears, acts like the planet gears. It consists of alternating sections of ferromagnetic and non-magnetic material and uses a principle called flux modulation to allow all of the magnetic poles in the sun and ring to engage with one another in a way that produces a gear ratio. This full engagement of all the magnetic poles enables the CMG to have higher torque density than other embodiments of magnetic gearing. Further improvements on the CMG's torque density were made by using Halbach arrays in both the sun and ring gears. A Halbach array combines multiple magnets in a specific orientation pattern to produce a focused and nearly sinusoidal magnetic flux field without the use of ferromagnetic materials (Ref. 15). Li et al. (Ref. 7) numerically compared a CMG with Halbach arrays to other forms of concentric magnetic gearing and found it to have the highest torque density and lowest torque ripple. Currently, the CMG is the most developed form of magnetic gearing.

The CMG's principles of operation, particularly flux modulation, are explained by examining the components of the gear set and how they interact. Figure 1 shows a magnetic finite element analysis (FEA) simulation of a CMG's ring gear. In this example, the ring gear is a Halbach array composed of 24 pole pairs, which each contain 6 magnets. Arrows in the figure indicate the magnetization direction of each magnet. The closed loops indicate the paths taken by magnetic flux. The radial component of magnetic flux density is represented by color, where blue is inward and red is outward. As shown by the simulation, the array produces a circumferentially-periodic flux pattern inside the ring and very little flux outside of it. The periodicity of the flux is controlled by the number of magnetic pole pairs in the ring. Here, the fundamental wavelength, or period of repetition, is 15° or $360°/24$.

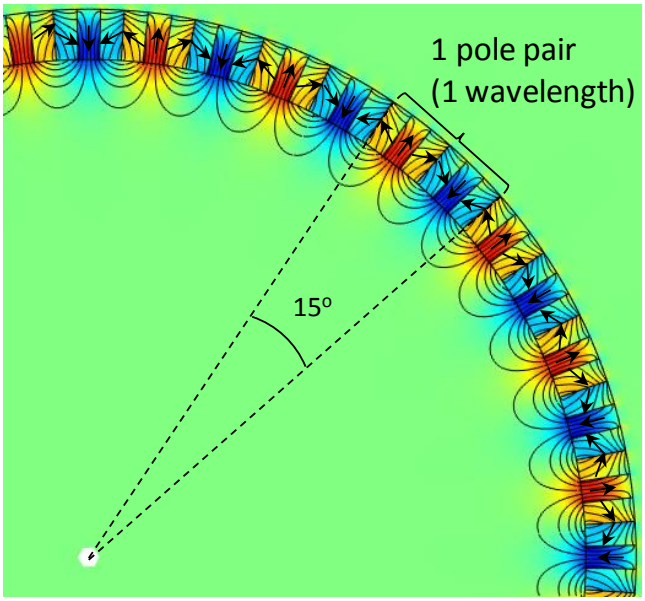

Figure 1: Magnetic flux density simulation of a Halbach ring gear.

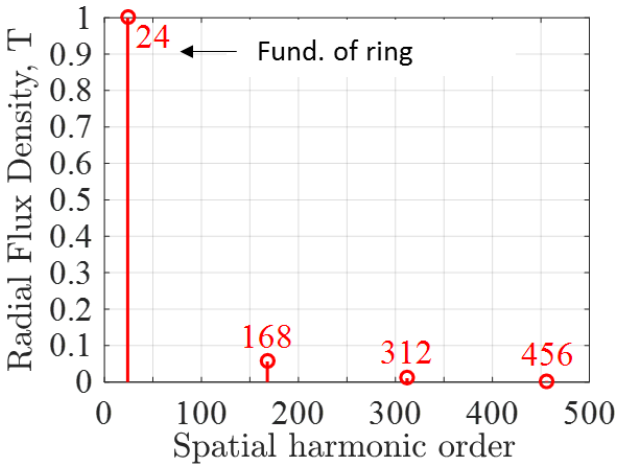

Figure 2: Radial magnetic flux density near the inner surface of the ring; from the fundamental spatial harmonic (24), the appreciable higher harmonics occur at integer multiples of the total number of magnets in the full circular array (144) (Ref. 15).

[a] Torque density is historically the metric used to quantify magnetic gearing. This is in contrast to the aerospace gearing industry, which generally uses specific torque.

In Figure 2, the radial component of the magnetic flux density near the inner surface of the ring gear is depicted in the order domain. For clarity, only the non-negligible points are shown. The flux density is normalized by the fundamental spatial harmonic of this ring gear, which is shown to be of the 24**th** order, corresponding to 360°/15° and the 24 pole pairs comprising the ring. No significant higher harmonic flux density is observed, indicating a smooth sinusoidal pattern. The magnitude of the higher harmonic content is inversely related to the number of magnets in each pole pair.

The magnetic simulation in Figure 3 demonstrates the effect of adding a flux modulator to the simulation of the ring gear from Figure 1. Here, the flux modulator consists of 30 evenly distributed ferromagnetic pieces, which are referred to as pole pieces. For clarity, only the inward oriented magnets are denoted. Compared to the ring gear alone (Figure 1), the presence of the flux modulator causes some of the flux produced by the ring gear to project inside the flux modulator with a wavelength of 60°, or 4 times that of the ring. This modulated flux waveform corresponds to a spatial harmonic order of 6. This is examined further using the order domain plot of Figure 4, which depicts the radial flux density near the inner surface of the modulator. The spectrum includes strong 6th and 24th order components, indicating only partial modulation of the ring's fundamental 24th order harmonic. Compared to Figure 2, the modulator also introduces unintended higher harmonic content; this is assumed to be caused by the nonlinear permeability and discrete geometry of the pole pieces.

In order to understand how the gear ratio of a CMG is produced, it is important to understand how the modulated 6th order harmonic propagates as the ring gear is rotated. While the modulator is fixed, if the ring in Figure 3 is rotated by one period (15°) so that pole piece A is centered on magnet 2, rather than magnet 1, the system reaches an identical position to that depicted. Thus, the modulated waveform must also rotate a full period (60°), or 4 times further than the ring.

A magnetic simulation of the complete CMG is shown in Figure 5. All three components – sun, modulator, and ring – are included. Generally, in order for torque to be created by two interacting spatial-harmonics, their harmonic order has to be the same. Here, the sun is an outward facing Halbach array with 6 pole pairs (and 10 magnets per pole pair) producing a 6th order field that engages with the modulated ring field. With the sun engaged to the modulated ring field, it will operate at a higher speed than the ring, thus establishing the gear ratio. Conversely the sun's field is modulated to the 24th order to engage with the ring's fundamental field. Consequently, the sun and ring are magnetically coupled and torque can be transferred. This coupling can be seen by the flux lines that loop through both components. A set of coupling flux lines are highlighted in blue for emphasis. Other flux lines that do not loop through both components do not create coupling and are called leakage flux. Example leakage flux loops are highlighted in red. Minimizing the leakage flux and maximizing the coupling flux in a CMG is key to creating high torque capacity.

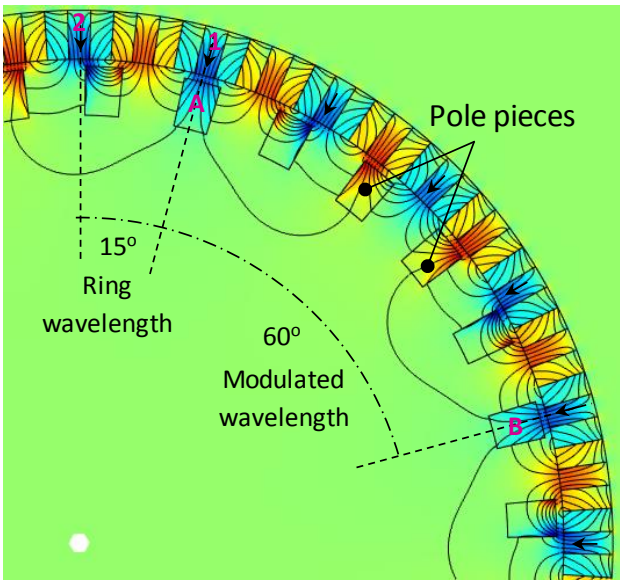

Figure 3: Flux density simulation of Halbach ring gear with modulator.

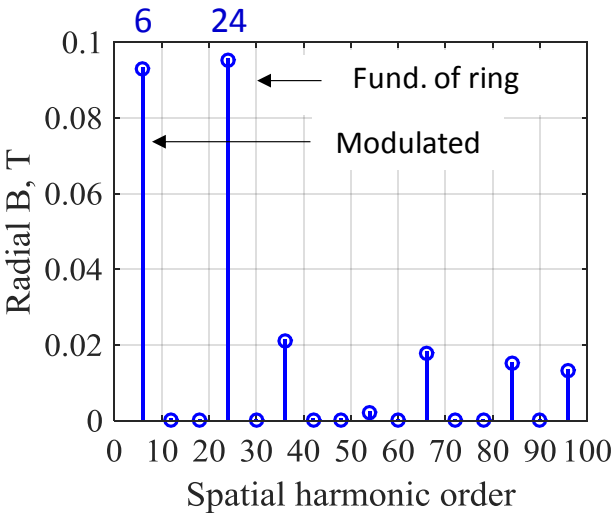

Figure 4: Radial magnetic flux density near the inner surface of the modulator.

Figure 6 shows an order domain plot of the radial flux in both the inner and outer magnetic gaps of the CMG. Here we see the intended 6th order harmonic in the inner magnetic gap and 24th harmonic in the outer magnetic gap. However, the presence of the Sun's 6th order harmonic in the outer magnetic gap, as well as some higher-harmonic content indicates imperfect modulation.

The fundamental relationship that enables commensurate spatial harmonics to be produced by the three components is

$$q = p_l + p_h \quad (1)$$

where q is the number of modulator pole pieces, and p_h and p_l are the number of pole pairs on the high and low speed rotors, respectively (Ref. 8). Like a planetary gear set, any of the members of the CMG may be fixed and the other two used as rotors. The gear ratio of the CMG is defined by the relative number of pole pairs in the same way that the relative number of gear teeth defines the gear ratio in mechanical gearing. If the modulator is the fixed member, the gear ratio is define by the pole ratio, according to,

$$G_1 = p_l/p_h, \tag{2}$$

and the rotors spin in opposite directions. If instead, the ring is fixed, the ratio is slightly higher,

$$G_2 = 1 + p_l/p_h = q/p_h, \tag{3}$$

and the rotors spin in the same direction.

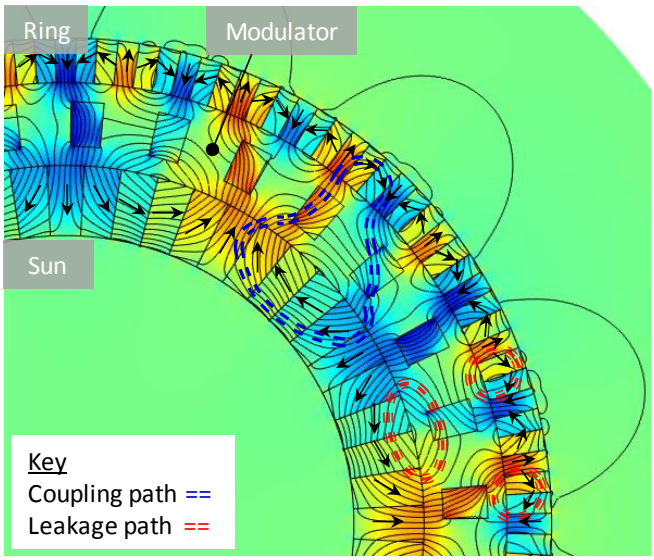

Figure 5: Flux density simulation of CMG

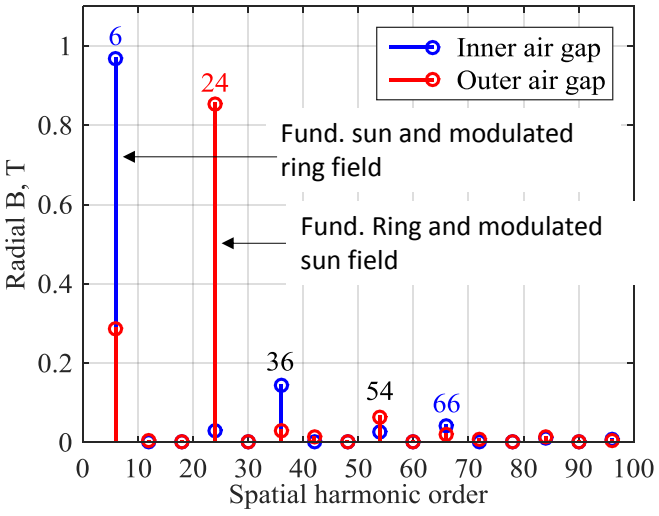

Figure 6: Radial magnetic flux density in the inner and outer magnetic gaps of the CMG.

PROGRESS OF TECHNOLOGY DEVELOPMENT AT NASA

Starting in 2017, NASA launched a 2-1/2 year project to establish a core competency in magnetic gearing technology and help advance the state of the art for aerospace applications. Initially, the technology is being developed towards small electrified aircraft as a means to enable the use of geared motors without the lubrication, noise or maintenance issues associated with mechanical gearing. In order to make magnetic gearing feasible, progress is needed to improve specific torque and enable high speed operation. The project was therefore structured into three phases. The first phase was recently completed, and it focused on gaining a core understanding of the technology and increasing specific torque. Results from this phase will be summarized in this section. Phases two and three will respectively focus on enabling high speed operation and motor/gear integration. These topics will be discussed in the next section.

Objectives and scope of phase 1

The objective of phase one was to gain a core understanding of the technology and increase the specific torque. To accomplish this objective, two prototypes were built. The first (PT-1) was developed quickly with the goal of gaining practical magnetic gear design and manufacturing experience. The second (PT-2) was developed more methodically with the goal of maximizing specific torque.

The prototypes were both loosely tailored to NASA's X-57 Maxwell aircraft's high-lift propulsors. Potentially significant benefits to X-57 could be realized by replacing each low-duty-cycle, high-lift motor with a magnetic gear and smaller motor. The prototypes were restricted to fit within a 152 mm outer diameter and mechanically designed to support an output speed of 4500 rpm, matching the X-57 high lift motor's requirements. A gear ratio of 4 was selected to significantly reduce the motor's torque, thereby enabling a significant reduction in its mass.

Standard magnetic materials were used in both designs. Neodymium N52 magnets were selected for use in the magnetic arrays of both the sun and ring gear, because of their high remanent flux density. Non-oriented, electrical steel laminations (HF-10, 0.254 mm layer thickness, with C5 coating) were used to compose the pole pieces of the modulator, because this is a standard practice to mitigate eddy current power loss.

All of the structural components for both prototypes except for the bearings, shafts, and screws were produced using 3D printing to reduce lead times and enable rapid prototyping. The structures were printed from a nylon based material that was reinforced in select locations with continuous carbon fiber strands. This capability enabled structurally-sound components to be made that were lightweight and had high strength where required.

In both of the prototypes, the ring gear was selected as the stator, the sun as the input, and the modulator as the output. The sun was chosen as the input because its smaller size makes it the most practical choice for the rotor that has a smaller pole count. The modulator was selected as the output because the alternative choice (i.e., the stator) leads to cantilevered designs that require the modulator structure to support the gear's bearing loads from only one axial side. Selection of the ring as the stator enables the use of the entire outer surface for mechanical support. Additionally, taking the modulator as the output provides a higher gear ratio for a given pole configuration, as discussed in the previous section.

In the following sections, the design of each prototype will be discussed followed by a summary of the technology advancement achieved through phase one of this project.

Design of prototype 1

The design of PT-1 was driven by the decision to use off-the-shelf magnets to produce the ring and sun gears' Halbach arrays. This decision was made to increase the manufacturing speed of PT-1 by eliminating the lead time for custom magnets. As shown in the magnetic configuration graphic in Figure 7, magnets with a square axial cross section were chosen to allow both the ring and sun gear to use 4-magnet Halbach arrays constructed from a single magnet type. A pole pair count of 13 was selected for the ring gear so that 6.35 mm (0.25 in) square magnets could be used while staying within the diametric constraint. A pole pair count of 4 was selected for the sun gear so that 12.7 mm (0.5 in) square magnets could be used while maintaining about 10 mm of space between the sun and the ring for the modulator. Consequently, the modulator needed to have 17 pole pieces based on equation (1). This created a 4.25 to 1 gear ratio, according to equation (3). The axial length of the magnetic components (stack length) was selected to be 25.4 mm (1.0 in), because both 6.35 mm and 12.7 mm square magnets were commercially available in that length.

A limited 2D electromagnetic FEA analysis was conducted to design the pole pieces of the modulator to maximize the specific torque of the gear. Only two variables – inner and outer pole piece span angles, as defined in Figure 1 – were studied; these span angles are the angles subtended by the inner and outer surface, respectively, of each modulator pole piece. The initial value used for both of these angles is defined by: $\alpha = 360°/(2 \cdot q)$, where α is the span angle. This resulted in an initial span angle of 10.6 degrees. The electromagnetic analysis led to the selection of a slightly smaller inner span angle (10 degrees) and a larger outer span angle (14 degrees). This design produced a 2D FEA simulation torque of 53 Nm with an active mass of 1 kg once all of the manufacturing considerations were taken into account.

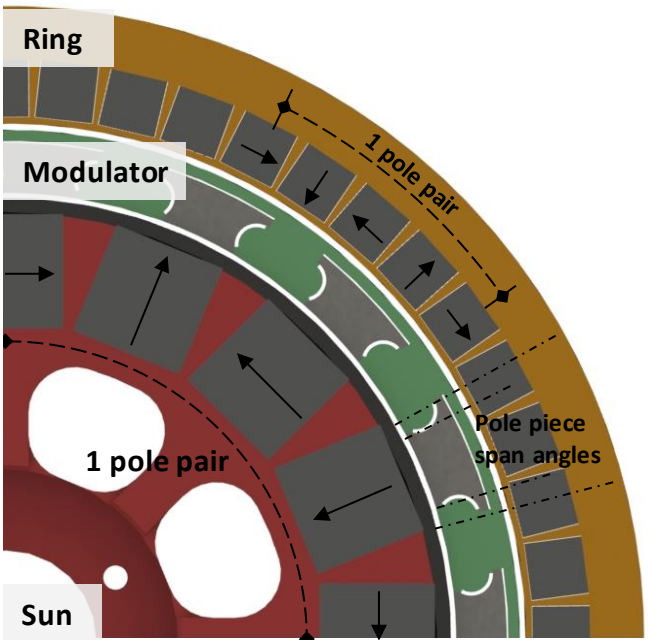

Figure 7: Magnetic configuration of PT-1

Manufacturing of prototype 1

Most of the manufacturing of PT-1 was done in-house; however, the pole pieces were procured from an external shop. The electric steel laminations were laser cut into the pole piece 2D geometry, annealed, and then stacked to length with thin layers of glue in-between each layer. The stacking process required the use of guide pins. A concave feature had to be added to both sides of each pole piece, as shown in Figure 7, to interface with these pins. The pole piece manufacturing process took about a month. It was by far the longest lead time of any component of the gear. In an effort to reduce this lead time, an alternate process was tried, where the pole pieces were cut from a large, pre-stacked sheet (30 x 30 cm) of the electrical steel laminations using wire electrical discharge machining. This approach was considerably faster, but caused several delaminations of the pole pieces and electrical shorting between the individual laminates. It was found that the shorting could be eliminated by either sanding or chemically etching the cut faces, but working with the delaminated pole pieces was cumbersome.

Significant manufacturing issues occurred because of the use of 3D printed plastic for the major structural components of the gear. The most prominent of these issues was printing accuracy. The specific nylon material used did not machine well. Therefore, every part had to be printed within the required tolerances for assembly of the gear. Achieving exact dimensions with 3D printed plastic is difficult due to the temperature variations undergone by the plastic in the printing process and the limited precision of most 3D printing machines. In order to mitigate these tolerance issues, multiple test prints were made with varied interface dimensions until the process produced parts within tolerance. Even with this strategy implemented, the nominal sizes of the physical gaps between the sun and modulator (0.5 mm) and between the ring

and modulator (0.71 mm) were too small and there was some rubbing between these members.

Assembly of PT-1 also proved to be difficult because of the use of 3D printed structures. The bodies of the sun, ring, and modulator, without all of their corresponding magnetic components inserted, were not stiff enough to withstand the magnetic forces that occurred during assembly. This lack of stiffness led to two failed attempts at assembly of the gear; in each case, one of the 3D printed members deformed past its structural limit as the magnetic elements were inserted. Based on this lesson, the sun, ring, and modulator were fully assembled as separate components prior to assembly of the full gear. This method still had difficulties as the sun, ring, and modulator were magnetically attracted to one another, making it difficult to establish concentricity between them. In the end, shims were required to keep the components aligned during assembly until all of the parts were properly bearing supported. A photograph of the fully assembled prototype is shown below in Figure 8.

Figure 8: Photograph of PT-1

Design of prototype 2

PT-2 was developed with the goal of maximizing specific torque. To accomplish this, PT-2 was not limited to off-the-shelf magnets like PT-1 was. Thus, PT-2 had a much more open design space. An iterative and incremental design process, depicted in Figure 9, was developed to explore this design space and converge on a design for PT-2.

The gear was broken into its subcomponents and simulated individually. This provided a more fundamental understanding of the subcomponent behaviors. Subcomponent studies started with sun gear and ring gear Halbach array simulations. Then, the modulator was simulated with the sun and ring separately. The understanding gained from these studies was then used to guide full gear simulations, which were aimed at maximizing specific torque. Finally, a mechanical design was developed based on the best electromagnetic geometry. This process was intended to be iterative with the understanding gained in each step fed forward to the next step and back to previous steps. Due to time constraints on phase 1 of NASA's project, only one iteration was completed prior to PT-2 being designed; however, this process is being continued in phase 2 of the project, with additional iterations of each step.

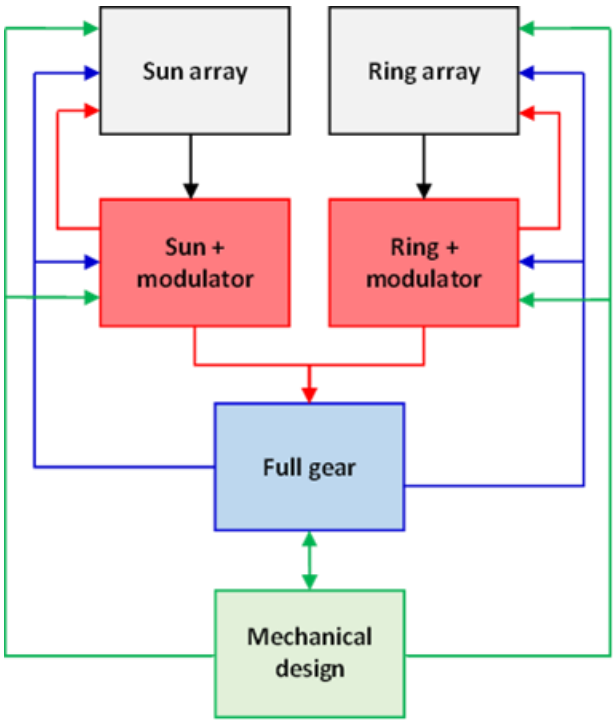

Figure 9: Process used to design PT-2 for maximum specific torque

In the following sections, lessons learned in the first iteration through this process and the design of PT-2 will be discussed.

Ring gear and sun gear Halbach array studies

Parametric studies were performed on both the sun gear and ring gear Halbach arrays with a focus on understanding design trends for maximizing the fundamental harmonic of specific flux produced by the arrays. A 2D magnetic FEA model was developed that included a nonlinear demagnetization model for the N52 magnets. By taking advantage of magnetic symmetry, only half of an array length, or the circumferential distance between pole pairs, was simulated to reduce computation time. The diameters of the arrays were set based on estimates of how big the sun and ring gears could be in a magnetic gear for the X-57's high-lift propulsors. The outer diameters selected for the ring and sun were 139.7 mm (5.5 in) and 114.3 mm (4.5 in), respectively. As shown in the magnetic configuration graphic in Figure 10, magnets shaped like annular wedges were used for all simulations in order to maximize the percentage of magnet material in the arrays. Parametric sweeps were performed by varying the number of

magnets in each array and the array's circumferential length and radial thickness.

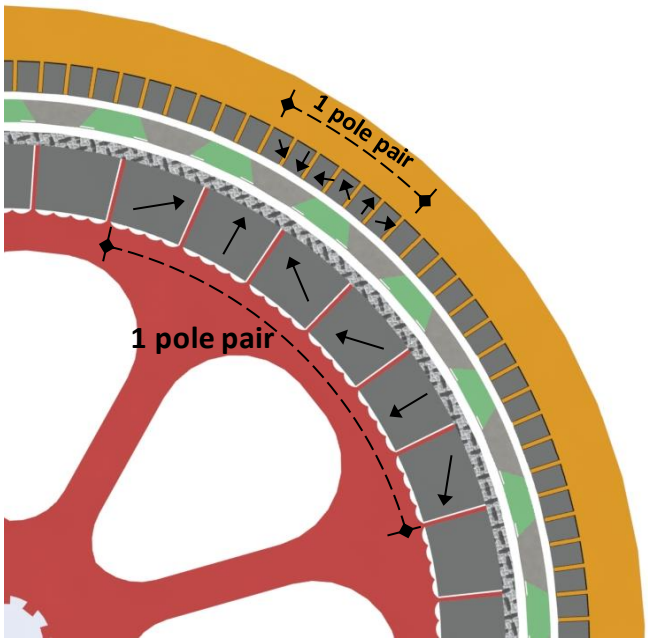

Figure 10: Magnetic configuration of PT-2

The results of the study showed that the specific flux increases as (1) the radial thickness is reduced, (2) the circumferential length of each pole pair is reduced, and (3) the number of magnets per pole pair increases. These trends are consistent with the analytical equations developed by Halbach for Halbach arrays (Ref. 15). The demagnetization model used for the magnets had no effect on these trends because, although demagnetization occurred in all simulations, it was limited to localized regions of the magnets.

Based on the results of this study, 6-magnet arrays and pole counts of 6 and 24 for the sun and ring gears, respectively, were used for all subsequent steps of the design process. Selection of 6-magnet arrays was based on the simulation results and manufacturing considerations. Magnet counts greater than six provided only incremental benefit, but increased the total number of magnets to assemble and the number of magnet types that needed to be produced. The pole counts were selected based on manufacturing and array length considerations. Smaller array lengths increase the specific flux of an array by reducing the distance, and thus magnetic reluctance, between neighboring poles. In practice, there is a limit to this trend, because the reduction in array length must be accompanied by a reduction in the magnetic gap to ensure that the flux crosses the gap to interact with the other magnetic components and produce torque. Hence, there is an optimal array length because there is a minimum achievable magnetic gap. The ideal pole pair counts for PT-2 were greater than the number selected for PT-1. Even pole counts were selected to enable the use of symmetry for computation speed in the next steps of the process.

Modulator studies

Parametric studies of the modulator were conducted to identify design trends for maximizing the specific flux of the fundamental and modulated harmonics produced by an array and modulator pair. Both the ring-modulator and sun-modulator pairs were studied. For each respective study, the fundamental harmonic of the array being simulated was evaluated in the magnetic gap between the array and modulator, whereas the modulated harmonic was evaluated on the side of the modulator that was furthest from the array. The modulated harmonic has the same spatial harmonic order as the number of pole pairs in the gear that it would couple with. Thus, the fundamental and modulated harmonics are related by the gear ratio in equation (3).

Studies were performed using a 2D FEA. The nonlinear demagnetization model was again used for the magnets, and a nonlinear magnetic flux density versus field strength (B-H) curve was used to define the magnetic response of the electrical steel pole pieces. Magnetic symmetry was again taken advantage of to limit the simulated arc length to the arc length of one sun gear pole pair. Array pole pair and magnet counts were held constant, as stated in the Halbach array simulation section. The outer diameter of the ring and sun arrays were again held at 139.7 mm (5.5 in) and 114.3 mm (4.5in). Parametric sweeps were performed on array thickness, pole piece thickness, and pole piece span angles.

The only significant and conclusive trend found in this study was that smaller pole piece thickness produced larger modulated specific flux. This trend is largely driven by reduced pole piece mass, but small increases in the magnitude of the modulated flux harmonics were also observed. There is a limit to this trend in specific flux because the modulation effect is lost below a pole piece thickness threshold. A further explanation of this minimum thickness will be provided in the next section. Conclusive trends on the effects of pole piece span angles and array-to-pole-piece thickness ratio could not be determined with the data collected in this first iteration of the overall design process.

Full gear simulations

The full gear parametric studies had the objective of maximizing the specific torque of the gear's magnetic components. Mechanical component masses were not accounted for in this first design process iteration. The FEA model from the modulator study was used here, but with both arrays and the modulator simulated together. As before, the pole pair and magnet counts were held constant. In addition, the ring gear array's outer diameter was held constant at 139.7 mm (5.5 in). Parametric sweeps were performed on magnetic gap thicknesses, magnet thicknesses, modulator thickness, and pole piece inner and outer span angles. The results of the study reveal some important magnetic gear design trends.

It was observed that the specific torque of the gear is much more sensitive to the thickness of the magnetic gap between

the ring and modulator than it is to the thickness of the magnetic gap between the sun and modulator. Generally, reduced magnetic gaps increase the specific torque of a CMG by reducing the magnetic reluctance of the magnetic circuit that couples the three components (sun, modulator, and ring) and increasing the magnetic reluctance of the leakage circuits. The ring-to-modulator magnetic gap has a larger effect on the CMG's specific torque because the ring gear is more susceptible to pole-to-pole flux leakage due to the shorter distance (and lower reluctance) between its poles.

Increases in the thickness of one of the magnet arrays in the CMG always increased the overall torque of the gear, but decreased the torque per mass of that array. These competing trends can be explained by a trend from the array studies; with increases in thickness, an array produces more flux, but its mass increases faster so that its specific flux decays. In the CMG, when an array's thickness increases, the extra flux from that array results in more torque. Initially, the increase in torque is substantial and more than offsets the increase in CMG's mass. Eventually, the increase in flux (and torque) becomes minimal and the mass effect dominates, leading to reductions in the specific torque of the CMG.

It was found that for a given set of magnetic gaps and modulator design, there was always a set of optimum magnet thicknesses for the two arrays. This finding is the result of the above trend related to magnet thickness and the mass of the modulator. While the CMG's torque per magnet mass of a given array always decays with increases in that array's thickness, to maximize specific torque, a certain amount of magnet thickness is required to produce sufficient torque to counteract the modulator mass.

The ideal magnet thickness was always found to be larger for the sun gear than it was for the ring gear. The ring gear's higher susceptibility to leakage between its poles is one cause of this difference. Because the magnetic reluctance of the ring gear's pole-to-pole leakage circuit is lower than that of the sun, a higher percentage of the flux it produces leaks. Therefore, thicker magnets are more effective on the sun than the ring because more of the flux produced enters the coupling path and contributes to torque production. Also, the sun's array length is greater than that of the ring. So the sun's array must be thicker to be equally effective.

There was always an ideal modulator thickness to maximize specific torque. When the modulator's thickness reduces, so does its mass. For a given specific torque, this mass reduction lowers the required torque, which allows thinner arrays that produce less flux. The thinner arrays provide an additional mass reduction. Thus, the combined effect with reduced modulator thickness is higher specific torque but a lower total torque. There is a limit to this trend where the modulator becomes so thin that the magnetic gaps dominate the reluctance between the ring and sun gears and the modulator loses its influence on the magnetic flux path. This minimum modulator thickness depends on the thickness of the two magnetic gaps and the relative permeability of the steel used to make the pole pieces.

Mechanical design

Based on the results of the full gear simulation an initial magnetic configuration was selected as a basis for PT-2. An increased stack length of 50.4 mm (2.0 in) was selected to reduce the gears susceptibility to axial leakage compare to PT-1. The pole count of the ring gear was reduced to from 24 to 23 in order to remove magnetic symmetry and reduce the torque ripple of the gear (Ref. 16). Thin walls between magnets were added to enable assembly of the sun and ring gear arrays and torque transmission. The magnetic gap between the sun gear and the modulator was increase by 30 percent to allow for the use of an off the shelf carbon fiber hoop for magnet containment. With these design changes taken into account the modulator thickness, magnet thickness, and modulator span angles were updated to re-optimize the specific torque of the gear. Overall the specific torque of the active components was 17% less than that of the initial magnet configuration.

Due to the small size of the modulator a unique squirrel cage-like structure was developed to contain the pole pieces. This structure was enabled by the use of the same 3D printed, fiber reinforced, nylon material. It was designed in order to avoid using hoops, which would have increased the magnetic gap, to contain the pole pieces radially. However tabs had to be added to the inner radius of the pole pieces to enable the structure. The pole pieces were redesigned to maximize the gear's specific torque with these tabs included. The modified pole piece design led to an additional 4% specific torque reduction.

The final 2D prediction of specific torque for PT-2 is 178 Nm. Its active magnetic mass is 1.7 kg. PT-2 is currently being fabricated. A detailed design paper on PT-2 will be written once its fabrication and testing are completed.

Prototype performance and technology advancement

Performance characteristics of PT-1 and PT-2 are summarized in Table 1. The predicted specific torque for PT-1, based on 2D FEA, was 31 Nm/kg. Through geometric optimization of the magnetic circuit elements, PT-2 achieved a predicted specific torque of 61 Nm/kg or roughly double that of PT- 1.

Table 2 summarizes resultant magnetic configurations of the two prototypes. The major magnetic configuration changes that enabled an improved specific torque from PT-1 to PT-2 are:

1. The magnetic fill of the ring and sun gear's Halbach arrays was increased by using annular wedge magnets, rather than square magnets, which better fit the form factor of the CMG.

2. The number of magnets per array was increased from 4 to 6, resulting in each array having higher specific flux.
3. Radially-thinner and circumferentially-shorter, higher pole count, Halbach arrays were used, also increasing the array's specific flux.
4. The magnetic gap between the ring gear and modulator was reduced, resulting in reduced leakage between the poles of the ring.
5. Pole piece thickness was reduced, resulting in both increased flux coupling and reduced mass.

Table 1: **Performance of PT-1 and 2**

	PT-1	PT-2
Torque (Nm)		
2D simulation	53.0	178
Measurement	34.0	N/A
Mass (kg)		
Active	1.0 (59 %)	1.7 (59 %)
Structural	0.7 (41 %)	1.2 (41 %)
Total	1.7	2.9
Specific torque (Nm/kg)		
2D simulation	31	61
Measured	20	>40 (est.)

As shown in Table 1, the measured specific torque of PT-1 is 20 Nm/kg. This indicates that the 2D prediction overestimated PT-1's specific torque by 35 %. By applying this same factor to the simulation results of PT-2, its actual specific torque is estimated to be 40 Nm/kg. This is considered to be a low estimate of the actual specific torque of PT-2, based on the differences in 3D leakage effects that are expected between the two prototypes.

Table 2: Magnetic configurations of PT-1 and 2

	PT-1		PT-2	
Mech. / mag. diameter (mm)	141.0 / 129.0		154.0 / 140.5	
Mech. / mag. length (mm)	92.4 / 25.4		114.3 / 50.8	
Mag. aspect	0.20		0.36	
Gear ratio (-)	4.25		~4.83	
Magnet shape	Square		Annular wedge	
	Sun	Ring	Sun	Ring
No. magnets per array	4	4	6	6
Array length (mm)	70.0	29.7	59.1	18.7
No. pole pairs (-)	4	13	6	23
Array thickness (mm)	12.7	6.35	7.75	3.63
Physical gap (mm)	0.50	0.71	1.0	1.0
Magnetic gap (mm)	2.1	2.8	2.6	1.0
	Modulator		Modulator	
No. pole pieces	17		29	
Pole piece thickness (mm)	5.6		2.7	

Gerber, et al (Ref. 17) provided insight into how 3D leakage effects differ between designs. He reported that 2D FEA commonly overestimates torque by 20 – 40 %, primarily because it does not capture the leakage that occurs in the axial direction. Comparison of 2D and 3D magnetic gear simulations showed that the disparity in predicted torque reduces as (1) magnets get thinner, (2) pole pieces get thinner, and (3) the axial length of the gear gets larger relative to its diameter. These changes relate to reducing the reluctance of the coupling path relative to the axial leakage path. Table 2 shows that PT-2 has made improvements over PT-1 in all three of these areas. Therefore, the difference between the 2D prediction and the actual specific torque should be much less than 35 %. As a result, 40 Nm/kg is considered to be a conservative estimate of PT-2's specific torque.

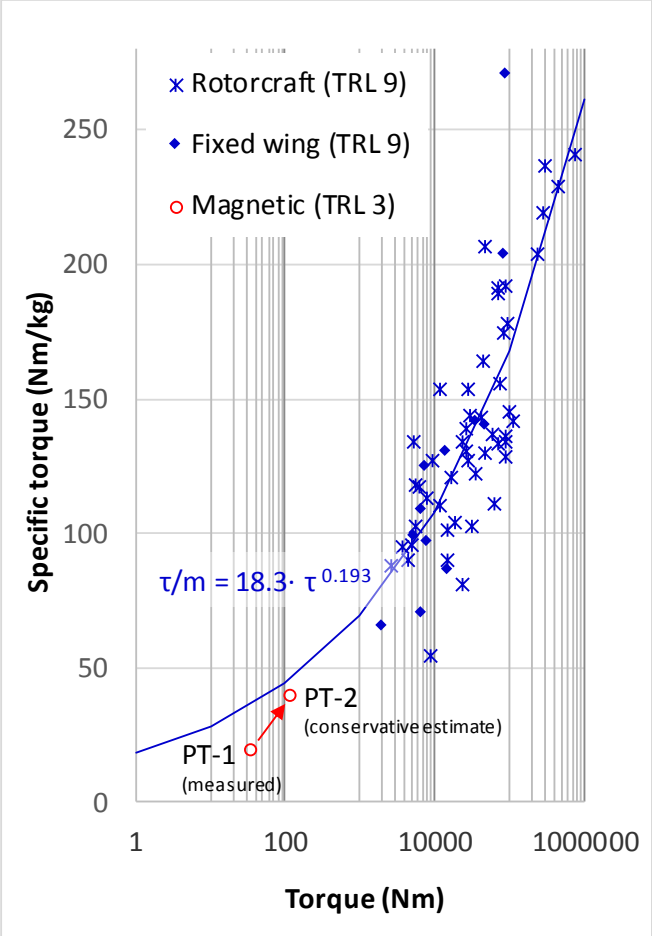

Figure 11: Specific torque of TRL 9 aircraft transmissions and TRL 3 CMG prototypes

For perspective, the specific torque of these magnetic gear prototypes is plotted vs. torque in Figure 11, along with 61 aircraft transmissions (49 rotorcraft and 12 fixed wing aircraft), as well as a trend line that fits the aircraft data. The transmission data set was published previously (Ref. 10), in a different form, for mass estimation. The mass values used to compute specific torque include both the gearbox and lubrication system. The aircraft transmissions range from 55 to 272 Nm specific torque, in comparison to the magnetic gear

prototypes that are 20 and 40 Nm/kg. However, the trend line shows that the specific torque of the aircraft transmissions drops significantly as torque is reduced. The conservative estimate for PT-2's specific torque is within 13 % of the aircraft transmission trend line at its torque level (116 Nm).

This observation indicates that magnetic gearing may be more competitive with mechanical gearing for relatively low torque applications, such as for driving the relatively small rotors used in some distributed propulsion eVTOL. More information is needed, however, to clarify the range of torque where magnetic gearing may be comparable. First, additional data on mass-optimized mechanical transmissions in the lower torque range is needed to verify or modify the trend. Second, the technology readiness level (TRL) of the magnetic gearing technology needs to be elevated. The prototypes produced are considered TRL 3; essentially experimental proof of concept. Changes in their structures will be required for heat transfer, mechanical endurance, and systems integration. These changes could have a significant impact on mass, as structures account for 40 % of the total mass in the prototypes developed. Another key point is that magnetic gear torque will be reduced with increased speed if significant eddy currents are generated. This issue will be discussed further in the following section on future work. Finally, to know how magnetic gearing compares at other torque levels, additional specific torque - optimized prototypes or scaling laws are needed.

There is also room for further improvement of CMG specific torque. Magnetic circuit optimization was limited by the structural design and manufacturing constraints. Magnetic gap sizes ran into the limitations of the 3D printing manufacturing process used. The inner magnetic gap was further limited by the magnetic containment hoop. Finally, the features added to the pole pieces that enabled mechanical integration with the modulator also reduced specific torque. New designs and manufacturing process that overcome these issues would open the design space and provide increased specific torque.

FUTURE WORK

Phase 2 of NASA's magnetic gear project will focus on making magnetic gears competitive with traditional gearing at the high speeds required for aerospace applications. Phase 3 will focus on integration of magnetic gears with electric motors. NASA's Revolutionary Vertical Lift Technology (RVLT) Project's eVTOL vehicle concepts will be the targeted applications for this continued technology development. In this section, first the eVTOL vehicle concepts and their gearing needs will be introduced and then the required magnetic gear technology development to satisfy these applications will be discussed.

Reference Vehicles

NASA's RVLT Project recently released three reference eVTOL vehicles designs, as detailed in Ref. 18 and illustrated in Figure 12. These vehicles are intended to represent a cross-section of the concepts emerging from the private sector, and are being used by NASA to focus and guide its eVTOL technology development efforts. There is single-passenger quadrotor vehicle, intended to operate as an *air taxi*, a 6-passenger side-by-side helicopter, for *vanpool* type operations, and finally a tiltwing aircraft, which would operate on a schedule like a traditional *airliner*. The release of these reference vehicles came after the completion of phase 1 of NASA's magnetic gearing project. These vehicles, however, will be target applications for NASA's continued development of magnetic gearing technology.

In these concepts, the rotors are either fully or partially driven by electric motors (EMs). Unlike most eVTOL vehicles being explored in the commercial sector, RVLT's concepts assume a gearbox is used to decouple the rotor and the EM's rotational speed. Propeller blade speeds are kept relatively low to minimize the noise associated with high propeller tip speed. The EM's rotational speed is assumed to be much higher, so that it can generate the required power with lower torque. Lower torque demand reduces the required electromagnetic loading, which enables the EM to be designed with lower mass and/or higher efficiency (Refs. 11 and 12).

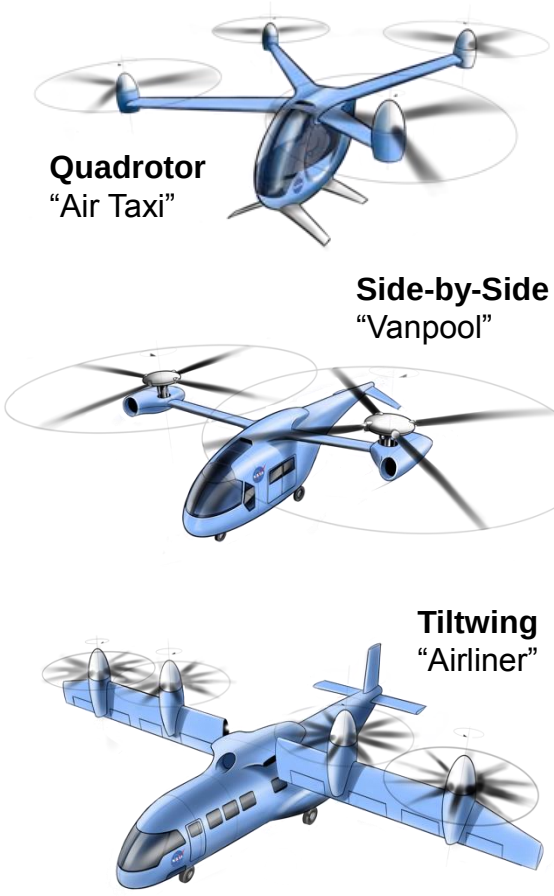

Figure 12: NASA's eVTOL reference vehicles

Table 3 displays the baseline propulsion configurations and gearing needs of each NASA reference vehicle. Here the load conditions for the gearing stages correspond to the aircraft in hover. The quadrotor has an electric propulsion system, where each rotor is driven by a geared EM. The load on the gearbox is quite low, 15.9 kW (21.3 hp), and it has a moderate gear ratio of 12.1.

Table 3: Baseline propulsion configurations, gearing needs, and hover load conditions for NASA's eVTOL reference vehicles

	Quad	Side-by-side	Tiltwing
Propulsion configuration:	Electric 4 rotors 4 EM	Par. Hybrid 2 rotors 2 TS, 1 EM	Turbo elec. 4 rotors 4 EM
Gear stage	EM-rotor	TS-rotor	EM-rotor
Ratio	12.1	Up to 140	9.3
Load (kW)	15.9	92.6	535
(rpm)	661	445	861
(Nm)	229	1987	5928
Gear stage	N/A	EM-rotor GB	Genset
Ratio		TBD	2.6
Load (kW)		73.2	2415
(rpm)		445	8000
(Nm)		1,569	2,883

The side-by-side has a parallel hybrid arrangement with each rotor driven by a geared turboshaft (TS) engine. In addition, a geared EM couples with the rotor gearbox (GB) through cross-shafting. This EM augments the power during hover conditions, and then during cruise the TS engines drive the EM as a generator to charge a battery. The TS gearing resembles that of a small helicopter; it has a moderate load power, 92.6 kW (124.2 hp), a very high reduction ratio, up to 140, and a 90 degree turn to transition from the horizontal TS engine to the vertical rotor shaft. It should be noted that the high gear ratio is based on the power turbine speed, without speed reduction within the engine. The EM gearing also has moderate load power, 73.2 kW (98.1 hp), as well as an undefined mechanism to regulate the supplied torque during hover and allow for power reversal during cruise. The gear ratio required for the EM will be based on the rotational speed at the stage where it's integrated in the rotor GB.

Finally, the tiltwing vehicle has a turboelectric propulsion system with a geared EM at each rotor. When converting from hover to cruise, the rotor's speed is reduced by 50 % as a result of lowering the EM's speed (as opposed to changing gear ratio). The EM to rotor gearing has high load power 535 kW (716 hp) and a moderate ratio of 9.3. Electric power is supplied by a geared TS to EM generation set (genset). The gearing used to connect the genset has very high load power, 2,415 kW (3,239 hp) and a low reduction ratio of 2.6.

Magnetic gearing could potentially provide a number of benefits over traditional gearing in these applications. These potential benefits include reduced maintenance costs, reduced noise, higher reliability, and improved loss of lubrication performance. However, the high input and output speeds associated with these applications are beyond the speeds that have been targeted for most magnetic gearing development. Additionally, these applications are much more sensitive to gearing weight than wind and automotive applications. Thus, for magnetic gearing to be viable for these applications, significant work is still needed to be done to produce a magnetic gear that has high specific torque and high efficiency at high rotational speeds.

Direction of future work

The focus of NASA's work on magnetic gears in phase 2 of the project will be on the development of the technology required to make magnetic gears efficient at the rotational speeds required for RVLT's eVTOL applications. The main loss mechanism for magnetic gears in high speed operation is eddy currents. Eddy currents result from time varying magnetic fields creating electrical fields inside conductive materials. They are a speed/electrical frequency dependent phenomenon that is prevalent in CMGs, because the sun and ring gears have different fundamental spatial harmonics that create high levels of time varying flux in each other and in the modulator. At the low rotational speeds of wind and automotive applications, eddy currents are not as big of a concern, so most of the magnetic gear development up to this point has not focused on mitigation of this loss mechanism.

Developing eddy current mitigation strategies will be a major focus of phase two of NASA's magnetic gearing work. How to optimize the design of CMGs to minimize the potential for eddy currents will be explored. Additionally, the use of alternative magnetic materials and laminated magnetic materials to reduce the effective conductivity of the active magnetic components in MGs will be investigated. Literature has also shown that eddy currents can be generated in the structural components of MGs if they are conductive and care is not taken to shield them from the magnetic fields of the gear. NASA plans to explore non-conductive structural material options to eliminate this potential loss mechanism without the use of magnetic shielding.

Considering that there will always be some level of power dissipation within the gear, heat dissipation will be another important topic. Without the use of lubrication, structural heat dissipation becomes more critical. The combination of requirements for structures to be electrically non-conductive to prevent eddy currents, but thermal conductive to remove heat, significantly reduces the material options. Thus, a research investigation into candidate materials and associated manufacturing processes is being undertaken.

High speeds raises issues with radial magnet and pole piece containment. Specific torque in the CMG is highly sensitive to magnetic gap size, it reduces the magnet array's ability to

drive the flux required to produce sufficient torque. At high speeds, radial containment of magnets and pole pieces becomes a problem that is typically solved with use of carbon fiber or titanium containment rings. Use of containment rings in the CMG requires increased magnetic gaps between the components to maintain physical gaps. NASA plans to look into alternative solutions for magnet and pole piece containment as they could lead to significant MG performance improvements at high speed.

Currently there is lack of test data on the high speed effects of magnetic gears. Therefore high speed testing will be done on PT-1 and 2, as well as future prototypes, to characterize torque, efficiency, vibration, and temperature as a function of speed.

CMGs lend themselves well to the EM-to-rotor stages of the quadrotor and tiltrotor RVLT Concepts. In line gearing makes sense for these stages. Their gear ratio requirements are also within the capabilities of a single CMG stage. In contrast, the side by side transmission has all of the challenges of a traditional helicopter; it requires a gear box that combines the power from two inputs, has shaft angle changes, and a high gear ratio. CMG's are not suitable for power combination or angle change. High gear ratios for CMG's are also difficult, because they require high pole counts, increasing leakage and eddy current concerns. Multi-stage designs are possible, but this configuration hasn't yet been explored. Thus, new magnetic gear architectures will be required to make a magnetic gearing feasible for this type of application.

Phase 3 of NASA's magnetic gear project will focus on how best to integrate electric motors with CMGs. It has been established in the technical literature that an electromagnetic stator may be integrated with the magnetic circuit of a CMG to create what is called a psuedo direct drive (PDD). The combination of a motor and CMG into a single component can potentially reduce the complexity and mass of the drivetrain. Many different PDD configurations have been proposed in recent years (Refs. 7 and 8). In phase 3, these topologies will be explored for use in the EM-to-rotor stages of the quadrotor and tiltrotor RVLT concepts.

CONCLUSION

Magnetic gearing is an alternative to mechanical gearing, where torque is transferred through magnetic force as opposed to contact force. The technology has the potential to be used in aircraft applications, without the lubrication, noise, and maintenance issues associated with mechanical gearing. NASA has initiated a 2-1/2 year project to establish a core competency and advance this technology.

This paper summarized the progress made in the first six months of the project, where the torque-to-mass ratio (specific torque) of concentric magnetic gear (CMG) technology was examined. This was done through the development of two small-scale (< 152 mm diameter) prototypes. Prototype 1 (PT-1) was developed rapidly to gain an understanding of design and fabrication issues. Its predicted specific torque (2D finite element simulation) was 31 Nm/kg while its measured value was 20 Nm/kg.

A systematic design process was then developed and implemented for prototype 2 (PT-2) to maximize its specific torque. Its 2D predicted specific torque was 61 Nm/kg, or roughly double that of PT-1. Prototype 2 has not been completely assembled at this time, but its measured specific torque can be estimated by applying the reduction factor (35 %) observed between PT-1's simulation and experiment. Doing so results in an estimated value of 40 Nm/kg. This is considered to be a very conservative estimate because PT-2 has a much higher aspect ratio and it contains other magnetic circuit features that are expected to reduce its 3D flux leakage and thus the drop in performance between 2D prediction and experiment.

For comparison, several rotorcraft and fixed wing aircraft transmissions were shown to range from 55 to 272 Nm/kg, with the trend showing that the higher specific torque values correspond to higher torque transmissions. The specific torque for PT-2, conservatively estimated at 40 Nm/kg, is lower than all of these transmissions. However, it is very close to the trend (within 13 %) when extrapolated to PT-2's torque level (116 Nm). This indicates that, in the near term, the CMG technology may be viable for lower torque applications, such as emerging electrified vertical takeoff and landing (eVTOL) aircraft. One important caveat here is that the prototypes produced have very low technology readiness level. As more engineering considerations are taken into account, their mass may grow. At the same time, there is further room for magnetic circuit optimization.

With regard to the CMG technology, the following lessons were learned:

1. Maximizing specific torque is achieve by creating the highest flux coupling between rotors with minimal mass penalty. This is primary accomplished by creating high specific flux magnet arrays and a low mass magnetic circuit with minimal flux leakage.
2. Custom magnets are a key factor in creating magnet arrays with high specific flux. Custom shape enables arrays with high fill factor. Custom poling enables a free selection of magnet count.
3. On their own, cylindrical Halbach arrays increase in specific flux as they get radially-thinner, circumferentially-shorter, and have a higher pole count.
4. Increasing pole count has diminishing returns on specific flux. Six magnets per pole pair provides most of the benefit without excess complexity.
5. When engaged with the CMG, there is an optimal radial thickness for an array. The specific flux of the arrays improves as it gets thinner, but a minimum

thickness is required to produce sufficient flux (and thus torque) to offset the mass of the pole pieces.

6. There is an optimal pole piece radial thickness. Thinner pole pieces reduce leakage and mass, but past a certain point their modulation effect diminishes.
7. Smaller magnetic gaps between the arrays and pole pieces reduces flux leakage. Smaller magnetic gaps also enable the use of thinner magnet arrays and pole pieces.
8. The low-speed, higher pole count rotor is more sensitive to variation in the adjacent magnetic gap, because its poles are closer together and therefore more prone to leakage between poles.
9. It is paramount to plan for magnetic forces in the assembly process when designing the mechanical structure of the gear.
10. The size of magnetic gaps is limited by mechanical considerations, such as structural tolerances and features for magnet and pole piece containment. Thus, structural changes that enable smaller magnetic gaps can increase specific torque.

In order to motivate further technology development, the gearing needs for NASA's reference eVTOL aircraft were presented. One of the common factors is that operational speeds are higher than typically considered for magnetic gearing applications. Efficiency loss and heat production through the generation of eddy currents are expected to be the primary challenges. Mitigating of these issues to enable high speed operation will be the focus of the next phase in the project.

Author contact: Vivake Asnani vivake.m.asnani@nasa.gov Justin Scheidler justin.j.scheidler@nasa.gov, Thomas Tallerico thomas.tallerico@nasa.gov.

ACKNOWLEDGMENTS

This work was supported by NASA's Independent Research and Development Program and Revolutionary Vertical Lift Technology Project. The authors would also like to recognize Dr. Timothy Krantz for providing the aircraft transmission data.

REFERENCES

[1]Armstrong, C. G., "Power transmitting device," US Patent No. 687,292, 1901.

[2]Errichello, R., "Lubrication of Gears Part 1," *Journal of the Society of Tribologists and Lubrication Engineers*, Vol. 46, (1), Jan. 1990.

[3] Errichello, R., "Lubrication of Gears Part 2," *Journal of the Society of Tribologists and Lubrication Engineers*, Vol. 46, (2), Feb. 1990.

[4]Coy, J. J., Townsend, D. P., and Zaretsky, E. V., "Gearing," NASA Reference Publication 1152, 1985.

[5]Federal Aviation Administration, "Airworthiness Standards: Transport Category Rotorcraft," FAR 29.927(c), 2017.

[6]Scheidler, J. J., and Asnani, V. M., "A review of noise and vibration control technologies for rotorcraft transmissions," INTER-NOISE 2016 Conference Proceedings, pp. 3378-3389, Hamburg, Germany, Aug. 21 - 24, 2016.

[7]Li, X., Chau, K.-T., Cheng, M., and Hua, W., "Comparison of Magnetically-Geared Permeant Magnet Machines," *Progress in Electromagnetics Research*, Vol. 133, 2013, pp. 177 – 198.

[8]Tlali, P. M., Wang, R-J., and Gerber, S., "Magnetic gear technologies: A review," 2014 Intl. Conference on Electrical Machines, p. 544-550, Berlin, Germany, Sept. 2 – 5, 2014.

[9]Moore, M. D., and Fredericks, B., "Misconceptions of Electric Propulsion Aircraft and their Emergent Aviation Markets," Paper AIAA 2014-0535, 52nd Aerospace Sciences Meeting, AIAA SciTech Forum Conference Proceedings, National Harbor, Maryland, January 13 – 17, 2014.

[10]Brown, G. V., Kascak, A. F., Ebihara, B., Johnson, D., Choi, B., Siebert, M., and Buccieri, C., "NASA Glenn Research Center Program in High Power Density Motors for Aeropropulsion," NASA TM 213800, 2005.

[11] Rahman, M.A., Chiba, A., and Fukao, T., "Super high speed electrical machines - summary," IEEE Power Engineering Society General Meeting Conference Proceedings, Denver, Colorado, June 6 – 10, 2004.

[12]Arkkio A., Jokinen T., and Lantto E., "Induction and Permanent-Magnet Synchronous Machines for High-Speed Applications," 8th International Conference on Electrical Machines and Systems Proceedings, Nanjing, P. R. China, September 27 - 29, 2005.

[13]Martin Jr., T. B., "Magnetic transmission," US Patent No. 3, 378, 710, 1968.

[14]Atallah, K., and Howe, D., "A Novel High-Performance Magnetic Gear," *IEEE Transactions on Magnetics*, Vol. 37, (4), July. 2001.

[15]Halbach, K., "Design of permanent multipole magnets with oriented rare Earth cobalt magnets," *Nuclear Instruments and Methods*, Vol. 169, 1980.

[16]Frank N. W. and Toliyat, H. A., "Gearing ratios of a magnetic gear for wind turbines," 2009 IEEE International Electric Machines and Drives Conference Proceedings, Miami, FL, pp. 1224-1230, 2009

[17]Gerber, S. and Wang, R-J., "Analysis of the end-effects in magnetic gears and magnetically geared machines," 2014 International Conference on Electrical Machines Proceedings, Berlin, German, pp. 396 – 402, Nov. 2014.

[18]Johnson, W., Silva, C., and Solis, E., "Concept Vehicles for VTOL Air Taxi Operations," American Helicopter Society Technical Conference on Aeromechanics Design for Transformative Vertical Flight, San Francisco, CA, Jan 16 – 19, 2018.